Models of nonequilibrium flow in porous medium

Kafi Ul Shabbir

June 21, 2023

Bachelor's Thesis
Supervisor: Oleg Izvekov
Presented on: 21.06.2023

Direction: 16.03.01 Technical Physics
Program: Aerospace Engineering
Department of Applied Mechanics
Phystech School of Aerospace Technology
Moscow Institute of Physics and Technology
Dolgoprudny

A part of this project was presented at the 65th All Russia Scientific Conference of MIPT.

Grant: RNF 23-21-00175
Author's email: kafiulshabbir@phystech.edu
Source code: https://github.com/kafiulshabbir/porus-fluid

Contents

Abstract

Simulation of two-phase flow in porous media has applications in oil recovery, hydrology, electricity production where pressurized water is passed through heated pipes and is transformed into steam, etc. We developed a network model which uses a new method of distributing phases in the nodes, it can be used to simulate models containing about 1000 pores within a few minutes on a personal computer. The results explain relaxation phenomena, in the model of imbibition where the saturation of a phase was calculated with respect to time, the wetting fluid enters the region with thinner radius. The flow rate when a tube contains meniscus after necessary derivation is given by a modified Poiseuille's equation. This produces n linear equations for a model with n nodes. The pressures at each node are the variables. Gaussian-elimination is used to solve the linear equations. Then the time step is decided and each meniscus in the tubes is displaced. The wetting fluid is distributed first in ascending order of the radius of the tubes. After this if there are more than two meniscus in a tube, the phases are combined such that the center of mass of the phases remain the same.

1 Introduction

1.1 Motivation

The subject of porous media represents an intensive research theme due to its practical applications in several fields, such as oil industry, chemical reactors, heat exchangers, thermal insulations, electronic cooling. [21]

1.2 Classical Continuum models

Continuum models of motion of multiple phases in a porous medium are widespread and useful, among them are Darcy's Law, Buckley-Leverett, etc.

Here permeability is only a function of saturation of one of the phase.

$$k = k(S) \tag{1}$$

Saturation is defined as the ratio between the volume occupied by a phase to the total volume of the void.

$$S = \frac{dV_w}{dV_{void}}$$

A feature of these classical models is that the relative phase permeability and capillary pressure are considered a function of saturation.

1.2.1 Darcy's Law

Darcy's law is a fundamental equation in fluid mechanics that describes the flow of fluids through porous media. It was formulated by Henry Darcy in 1856 and

has since become a vary important part of hydro geology, petroleum engineering, and other fields dealing with fluid flow in porous media. Darcy's law states that the flow rate Q of a fluid through a porous medium is directly proportional to the pressure gradient (ΔP) and the cross-sectional area A of the medium, and inversely proportional to the length L of the medium. Mathematically, it can be expressed as:

$$q = -\frac{k}{\mu}\nabla p \tag{2}$$

- q is the flow rate
- k is the permeability
- μ is the coefficient of viscosity
- ∇p is the pressure gradient

Darcy's law is widely used in the modeling and analysis of two-phase flow in porous media. Two-phase flow refers to the simultaneous flow of two immiscible fluids, such as gas and liquid, through a porous medium. In this context, Darcy's law can be extended to account for the flow of both phases.

One common application of Darcy's law in two-phase flow modeling is in the field of petroleum engineering, specifically in reservoir engineering. When modeling the flow of oil and gas in an underground reservoir, Darcy's law is used to estimate the flow rates and pressure distributions within the reservoir. By considering the relative permeability of oil and gas, the equation can be modified to account for the presence of two phases and their interactions [28].

Additionally, Darcy's law is often combined with other equations, such as the continuity equation and material balance equations, to create more comprehensive models for two-phase flow. These models can help predict the behavior of fluid flows in porous media, optimize production strategies, and estimate recovery factors in oil and gas reservoirs. [15]

1.2.2 Relative phase permeability

In multiphase flow in porous media, the relative permeability of a phase is a dimensionless measure of the effective permeability of that phase. It is the ratio of the effective permeability of that phase to the absolute permeability. It can be viewed as an adaptation of Darcy's law to multiphase flow.

For two-phase flow in porous media given steady-state conditions, we can write

$$q_i = -\frac{k_i}{\mu_i}\nabla P \tag{3}$$

for $i = 1, 2$

where q_i is the flux, ∇P is the pressure drop, μ_i is the viscosity. The subscript i indicates that the parameters are for phase i.

Relative permeability, k_{ri} is then defined as:

$$k_{ri} = \frac{k_i}{k}$$

where k is the permeability of the porous medium in single-phase flow, i.e., the absolute permeability. Relative permeability must be between zero and one.

In applications, relative permeability is often represented as a function of water saturation; however, owing to capillary hysteresis one often resorts to a function or curve measured under drainage and another measured under imbibition. [5]

1.2.3 Capillary pressure

Capillary pressure p_c is the difference between the average elementary volume fluid pressures.

$$p_c = p_{nw} - p_w \tag{4}$$

where p_c is the capillary pressure. p_{nw} is the pressure of the non-wetting phase. p_w is the pressure of the wetting phase.

1.2.4 Buckley-Leverett Theory

The Buckley-Leverett theory, also known as the fractional flow theory, is a mathematical model that describes the displacement of one fluid by another in porous media. It is widely used in the field of petroleum engineering

The Buckley-Leverett equation describes the fractional flow of one fluid phase (often called the displacing phase) as a function of the saturation of the other fluid phase (often called the displaced phase). Mathematically, the equation is given as:

The equation is given by:

$$f = \frac{(S_w - S_{wc})}{(1 - S_{wc} - S_{or})} \tag{5}$$

where:

- f is the fractional flow of the displacing phase.
- S_w is the saturation of the displaced phase (a fractional value between 0 and 1).
- S_{wc} is the critical water saturation (the saturation at which the capillary pressure becomes zero).

- S_{or} is the residual oil saturation (the saturation of oil that remains trapped in the rock after water flooding).

The Buckley-Leverett theory assumes that the fluids involved are incompressible and that the flow is governed by Darcy's law. The theory provides a framework to study the displacement of one fluid by another and predict the behaviour of the fluid fronts as they move through the porous medium. The key assumption in the Buckley-Leverett theory is that the fluids are flowing as distinct phases and that they exhibit capillary pressure and relative permeability characteristics. Capillary pressure represents the pressure difference between the two fluids at the fluid-fluid interface, and relative permeability describes the fractional flow of each fluid phase as a function of its saturation.

1.2.5 Leverett-J-function

The Leverett-J function, also known as the Leverett function or the J function, is a mathematical expression used in two-phase flow modeling to describe the capillary pressure-saturation relationship in porous media. It is an extension of the Buckley-Leverett theory.

The Leverett-J function relates the capillary pressure (Pc) to the saturation (Sw) of the wetting phase (usually water). The function describes how the capillary pressure changes with the saturation, providing insights into the fluid-fluid interactions and flow characteristics in the porous medium.

The Leverett-J function is expressed as follows:

$$J = \frac{\frac{dS_w}{dP_c}}{\frac{S_w}{P_c}} \tag{6}$$

where:

- J is the Leverett-J function.
- S_w is the saturation of the wetting phase (a fractional value between 0 and 1).
- P_c is the capillary pressure.

The Leverett-J function is used in two-phase flow modeling to estimate various parameters and analyze fluid displacement behavior. Some applications of the Leverett-J function include:

1. Estimating relative permeability
2. Predicting fluid displacement
3. Assessing reservoir connectivity
4. Optimizing enhanced oil recovery (EOR) techniques, it helps in understanding the capillary pressure distribution and identifying areas of bypassed oil

1.2.6 Empirical Model of Corey and Brooks

The Corey-Brooks Corey model, also known as the Corey-Brooks model or the Corey-Brooks-Kohoutek model, is an extension of the Buckley-Leverett theory.

The Corey-Brooks Corey model introduces an empirical function to describe the relative permeability curves for the two phases (typically water and oil) as a function of their respective saturation. The model assumes that the relative permeabilities are influenced by capillary pressure and can be expressed using power law relationships.

The relative permeability curves for the displaced (wetting) phase (typically water) and the displacing (non-wetting) phase (typically oil) are defined as follows:

The equations are given by:

$$k_{ro} = k_{ro_{\max}} \cdot (1 - S_w - S_{ro})^n$$
$$k_{rw} = k_{rw_{\max}} \cdot S_w^m$$

where:

- k_{ro} is the relative permeability of the non-wetting phase (oil).
- k_{rw} is the relative permeability of the wetting phase (water).
- $k_{ro_{\max}}$ and $k_{rw_{\max}}$ are the maximum relative permeabilities of the non-wetting and wetting phases, respectively.
- S_w is the water saturation (a fractional value between 0 and 1).
- S_{ro} is the residual oil saturation (the saturation of oil that remains trapped in the rock after water flooding).
- n and m are empirical exponents that govern the shape of the relative permeability curves.

The Corey-Brooks Corey model allows for the estimation of relative permeability curves for the wetting and non-wetting phases based on laboratory measurements or historical data. These curves are crucial in characterizing the flow behavior and predicting fluid displacement in porous media.

By incorporating the relative permeability curves into the Buckley-Leverett equation, the Corey-Brooks Corey model enables the simulation and prediction of two-phase flow behavior, such as fluid front movement and displacement efficiency, in reservoirs or aquifers. This information is valuable for optimizing production strategies, designing water flooding operations, and assessing the potential for enhanced oil recovery techniques [27].

1.3 Advanced Continuum models

The above models work as long as the characteristic time of the processes is much longer than the characteristic time of fluid redistribution in the capillary space.

For example, when the saturation changes rapidly, or when the porous medium has a structure such that the time of fluid redistribution is long (fractured-porous medium with blocks and cracks), the assumption that $K = K(S)$ is not sufficient and additional parameters are required.

There are a number of continuum models that take these effects into account. Among them Hasanizadeh [10] [12], Barenblatt [4] and Kondaurov [19]. The first two take into account not only saturation, but also the rate of saturation change.

From equation 2:

$$q = -\frac{k}{\mu}\nabla p$$

$$k = k(S, \frac{\partial S}{\partial t}) \tag{7}$$

The Kondaurov model, along with saturation, considers a special nonequilibrium parameter ξ, which should relax to an equilibrium value. [18]

$$k = k(S, \xi) \tag{8}$$

This parameter is related to S by the differential equation:

$$\frac{\partial \xi}{\partial t} = \Omega(S(t), \xi) \tag{9}$$

1.4 Model at the scale of pores

It is necessary to simulate the motion of phases at micro level, in order to better understand the models of nonequilibrium characteristics. There are a number of approaches to such modeling. For example Lattice Boltzmann Method or a direct Navier-Stokes calculation.

1.4.1 Lattice Boltzmann Method (LBM)

The Lattice Boltzmann Method (LBM) is a computational fluid dynamics (CFD) technique used to simulate fluid flow and solve complex fluid dynamics problems. It is particularly useful for modeling two-phase flow, where two immiscible fluids flow through a domain with interfacial interactions.

Unlike traditional CFD methods based on solving the Navier-Stokes equations, the Lattice Boltzmann Method operates on a mesoscopic scale and simulates fluid flow by modeling the behavior of particles (often referred to as "lattice cells") on a discrete lattice. It uses a kinetic approach to solve the Boltzmann equation, which describes the evolution of particle distribution functions [1].

The Lattice Boltzmann Method is advantageous for modeling two-phase flow because it naturally captures interfacial phenomena, such as fluid-fluid interfaces,

droplet dynamics, and interfacial tension effects. It can handle complex geometries and is capable of capturing mesoscale phenomena like droplet coalescence, breakup, and multiphase interactions [32].

The application of LBM in two-phase flow modeling involves the following steps:

1. Lattice Construction: The computational domain is discretized into a lattice structure.
2. Particle Distribution: These distribution functions evolve based on collision and streaming processes.
3. Collision and Streaming: The distribution functions undergo a collision step, where particles interact and exchange momentum and energy. After the collision, the particles stream to neighboring lattice cells based on predefined velocity directions.
4. Macroscopic Properties: Macroscopic fluid properties such as density, velocity, and pressure are calculated from the distribution functions.
5. Interfacial Effects: Interfacial phenomena, such as surface tension and interfacial forces, are incorporated into the Lattice Boltzmann Method.

1.4.2 Direct Numerical Simulation NAVIER-STOKES

Direct Numerical Simulation (DNS) is a computational technique used to solve the complete set of equations governing fluid flow without any turbulence modeling assumptions. It provides a detailed and accurate representation of fluid behavior by discretizing the governing equations in space and time and solving them numerically. DNS is particularly useful for studying turbulent flows, where turbulence models often introduce uncertainties and limitations.

By performing DNS of two-phase flow, researchers can gain insights into various phenomena and phenomena of interest, such as bubble or droplet breakup, coalescence, collision dynamics, and heat and mass transfer between the phases. DNS can also be used to investigate complex multiphase flows, such as bubbly flows, particle-laden flows, or flows with phase change [7].

The application of DNS in modeling two-phase flow offers several advantages:

1. Accuracy: DNS provides a high level of accuracy and resolves small-scale turbulent structures.
2. Detailed information: DNS captures detailed information about the flow, such as velocity profiles, vorticity, and pressure distribution.
3. Validation of models: DNS can be used to validate and improve existing turbulence models.
4. Design optimization: DNS helps in optimizing the design of various systems involving two-phase flows, such as heat exchangers, chemical reactors, and combustion chambers.

5. Fundamental understanding: DNS aids in developing a fundamental understanding of the underlying physics of two-phase flow.

1.4.3 Hybrid Models

A hybrid model, in the context of two-phase flow modeling, refers to a combination of different modeling approaches or techniques to capture the complexities and improve the accuracy of simulations. It involves integrating multiple models or methods, each designed to address specific aspects of the flow behavior, to create a more comprehensive and accurate representation of the system [23].

Here are a few examples of hybrid modeling approaches commonly used:

1. Coupling of Continuum and Discrete Models: This approach combines continuum-based models, such as the finite element method (FEM) or finite difference method (FDM), with discrete models, such as lattice Boltzmann method (LBM) or pore network models. Continuum models are used to capture the overall behavior of the flow field, while discrete models focus on capturing specific phenomena at a smaller scale, such as interfacial dynamics or fluid-fluid interactions. The coupling allows for a more accurate representation of complex flow behavior.

2. Multiphase Flow with Computational Fluid Dynamics (CFD) and Volume-of-Fluid (VOF) Method: In this approach, CFD methods are used to solve the Navier-Stokes equations and simulate the fluid flow, while the Volume-of-Fluid method is employed to track the fluid interface and capture the two-phase flow behavior. CFD provides detailed information on velocity and pressure fields, while VOF method accurately captures the shape and movement of the fluid interface.

3. Combination of Empirical and Mechanistic Models: Hybrid models can combine empirical correlations, such as relative permeability or capillary pressure models, with mechanistic models that describe fluid behavior based on fundamental principles, such as the Buckley-Leverett theory or Darcy's law. This allows for a more accurate representation of flow behavior by incorporating both empirical knowledge and physics-based understanding.

The specific formulas used in hybrid models depend on the combination of models and methods being employed.

The choice of the hybrid modeling approach and the formulas used depends on the specific objectives, computational resources available, and the level of accuracy required in capturing the two-phase flow behavior [26].

1.4.4 Upscalling Techniques

Upscaling techniques in two-phase flow modeling refer to methods that aim to represent the behavior of fluid flow at a larger scale, such as the reservoir scale, based on information obtained at a smaller scale, such as the pore scale. These

techniques are employed to reduce the computational cost and improve the efficiency of simulating two-phase flow in large-scale reservoirs or heterogeneous porous media [9], [29].

The application of upscaling techniques in two-phase flow modeling involves the following steps:

1. Characterization of Heterogeneous Media: The porous media are characterized at a fine scale, typically using methods such as core analysis, well logs. This provides information on the spatial distribution of rock and fluid properties, such as porosity, permeability, and saturation, at a small scale.
2. Selection of Upscaling Approach: Various upscaling techniques can be employed based on the nature of the porous media and the properties of interest. Some common upscaling approaches include arithmetic averaging, geometric averaging, and flow-based upscaling methods such as the streamline-based or multiscale finite volume methods.
3. Upscaling Equations: The upscaling technique involves deriving equations or relationships that connect the fine-scale properties to the coarse-scale properties. These equations capture the effective behavior of the flow variables, such as effective permeability or relative permeability, at the larger scale.
4. Coarse-Grid Simulation: Using the upscaled properties and equations, a simulation is performed at the coarse scale. This involves solving the governing equations, such as Darcy's law or the continuity equation, on a coarser grid that represents the larger-scale domain.

Some common formulas used in upscaling techniques for two-phase flow modeling include:

1. Effective Permeability: The effective permeability at the coarse scale is often computed using an averaging technique, such as arithmetic or geometric averaging, applied to the fine-scale permeability values. For example, arithmetic averaging is given by:

   The equation is given by:

   $$K_{\text{eff}} = \frac{1}{V} \int K \, dV$$

   where:

   - K_{eff} is the effective permeability.
   - K is the fine-scale permeability.
   - V is the volume of the representative elementary volume (REV) at the coarse scale.

2. Relative Permeability: The relative permeability at the coarse scale is derived based on the relative permeability curves obtained at the fine scale. Different upscaling approaches, such as the Brooks-Corey model or the Corey-Brooks Corey model, can be employed to obtain the effective relative permeability curves at the coarse scale.

3. Capillary Pressure: Upscaling capillary pressure involves relating the fine-scale capillary pressure-saturation relationship to the coarse-scale properties. Various methods, such as the Leverett-J function or a pore network-based approach, can be used to upscale the capillary pressure.

Upscaling techniques are essential for simulating large-scale two-phase flow systems, such as reservoirs, efficiently and accurately. They allow for the transfer of information from small-scale simulations to larger scales, thereby reducing computational costs while preserving the key flow behavior and properties. The choice of upscaling technique depends on the characteristics of the porous media and the desired level of accuracy in the simulation[22].

1.4.5 Network Models

Network models are much simpler to model and perform computations than direct Navier-Strokes calculations.

One of the earliest models, simulated the flow using a network of electrical resistors [8].

Simulation was also conducted using hour glass shaped model of tubes [2], where the average flow rate is given by the Washburn equation for capillary flow [30], the disadvantage is that the flow rate must be approximated for cylindrical tube while in the mode the capillary pressure varies as its position in the tube.

We developed a new network model, which differes from the other Network models, when more than 1 phase flows simultaneously into a tube, the wetting fluid is first distributed according to the ascending order of the radius of the tubes.

2 Theory

2.1 Porous body

Figure 1 is an example of two-phase flow in porous body. The wetting fluid, in this case - water displaces the non wetting fluid - air. The aim is to plot concentration of one of the phases with respect to time for a given region of the porous body, similar to [8]. In this work, we focus on the process of wetting fluid entering the region of finer pores, in our model denoted by thinner radius.

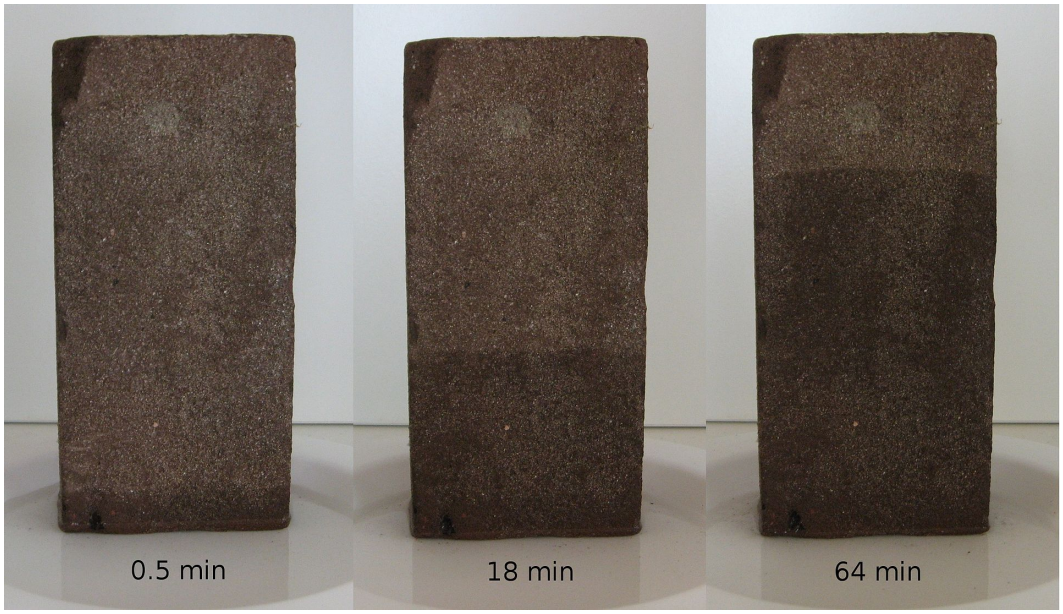

Figure 1: Water climbing against gravity through a porous medium. [31]

2.2 Viscosity

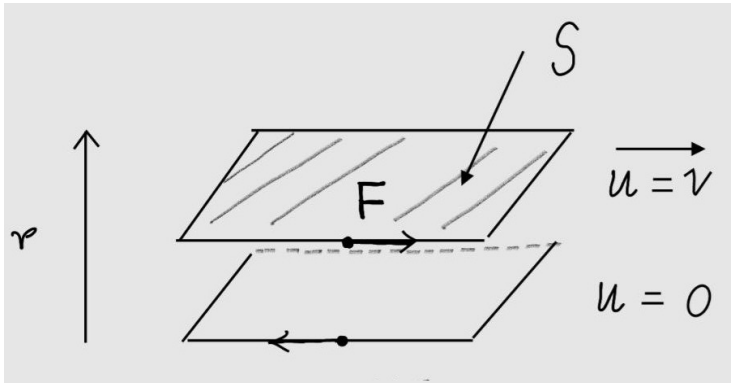

Figure 2: Force between two layers of viscous liquid

Viscosity is defined as,

$$\frac{F}{A} = \mu \left| \frac{dv}{dr} \right| \tag{10}$$

- F: shearing force on a surface of the layer, this force acts parallel to the surface plane.
- A: the area of the surface.
- μ: coefficient of viscosity.
- v: velocity of the flow parallel to the plane.

- r: coordinate perpendicular to the plane.

Dimension of viscosity,

$$[\mu] = \frac{[F]}{[A]}\frac{[r]}{[v]}$$

$$[\mu] = \frac{[ML/T^2]}{[L^2]}\frac{[L]}{[L/T]}$$

$$[\mu] = \frac{M}{LT} = \frac{kg}{m.s} \tag{11}$$

2.3 Volumetric flow rate through a thin tube

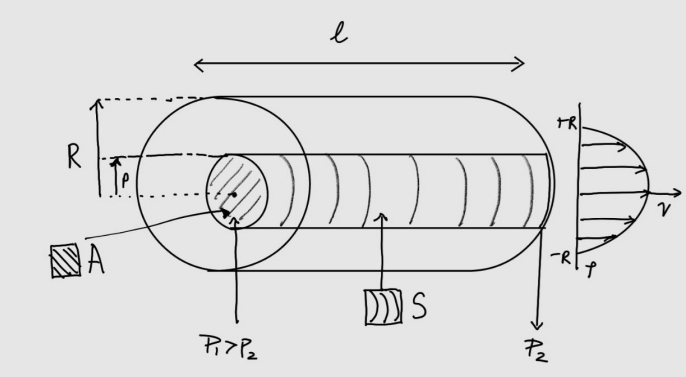

Figure 3: Flow through a thin tube

Rearranging 10, the viscous force is given by,

$$F_{vis} = A\mu\left|\frac{dv}{dr}\right| \tag{12}$$

The force due to pressure gradient, for a cross-sectional area S,

$$F_p = S\Delta P \tag{13}$$

For a laminar flow, the force due to pressure gradient is compensated by the viscous resistance in the opposite direction, which also means that the fluid does not accelerate.

$$F_p = F_{vis} \tag{14}$$

Substituting 12 and 13 into 14,

$$S\Delta P = A\mu \left|\frac{dv}{dr}\right|$$

The velocity is maximum in the centre, and zero at the boundaries. Which implies, that the velocity decreases with increasing radius.

$$\left|\frac{dv}{dr}\right| = -\frac{dv}{dr}$$

$$S\Delta P = -A\mu\frac{dv}{dr}$$

Substituting $S = \pi r^2$, and $A = 2\pi rl$,

$$(\pi r^2)\Delta P = -(2\pi rl)\mu\frac{dv}{dr}$$

$$(r)\Delta P = -(2l)\mu\frac{dv}{dr}$$

$$-2dv = \frac{\Delta P}{\mu l} r dr$$

$$-2\int dv = \frac{\Delta P}{\mu l}\int r dr$$

$$-2v + C = \frac{\Delta P}{\mu l}\frac{r^2}{2}$$

At $r = R$, $v = 0$

$$-2(0) + C = \frac{\Delta P}{\mu l}\frac{R^2}{2}$$

$$C = \frac{\Delta P}{\mu l}\frac{R^2}{2}$$

$$-2v + \left(\frac{\Delta P}{\mu l}\frac{R^2}{2}\right) = \frac{\Delta P}{\mu l}\frac{r^2}{2}$$

$$2v = \frac{\Delta P}{\mu l}\frac{R^2}{2} - \frac{\Delta P}{\mu l}\frac{r^2}{2}$$

$$v(r) = \frac{\Delta P}{4\mu l}(R^2 - r^2) \tag{15}$$

In order to find the volumetric flow rate Q in a tube, we integrate for each thin strip $2\pi r dr$

$$Q = \int_S v dS = \int_0^R v(r)(2\pi r)dr$$

$$Q = 2\pi \int_0^R v(r) r dr$$

Substituting $v(r)$ from 15

$$Q = 2\pi \int_0^R \left(\frac{\Delta P}{4\mu l}(R^2 - r^2) \right) r dr$$

$$Q = \frac{\pi \Delta P}{2\mu l} \int_0^R (R^2 r - r^3) dr$$

$$Q = \frac{\pi \Delta P}{2\mu l} \left[\frac{R^2 r^2}{2} - \frac{r^4}{4} \right]_0^R$$

$$Q = \frac{\pi \Delta P}{2\mu l} \left(\frac{R^4}{2} - \frac{R^4}{4} \right)$$

$$\boxed{Q = \frac{\pi}{8} \frac{\Delta P}{\mu l} R^4} \tag{16}$$

2.4 Capillary Action

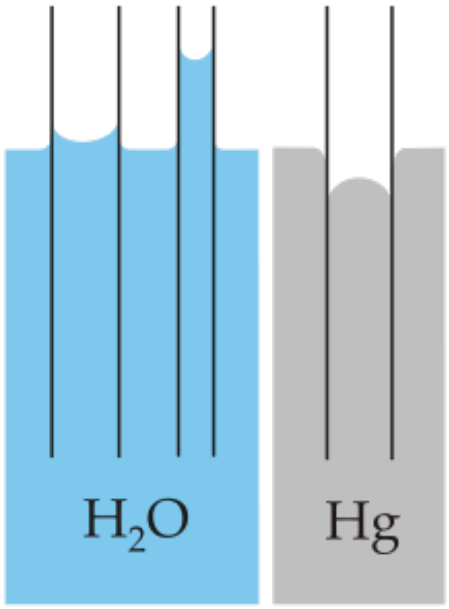

Figure 4: Showing capillary action of water (polar) compared to mercury (non-polar), with respect to a polar surface such as glass (Si–OH).

Let us apply this to our case, where the first node is filled with a fluid like water and the second node is filled with a fluid like air, and the our tube is similar to glass. Hence the meniscus will be oriented in a manner shown below.

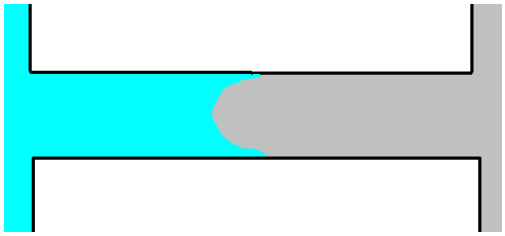

Figure 5: Orientation of meniscus, when one of its side is filled with wetting fluid while the other side is filled with a non-wetting fluid.

This causes the water to climb against gravity.

2.5 Flow rate in a tube containing 1 meniscus

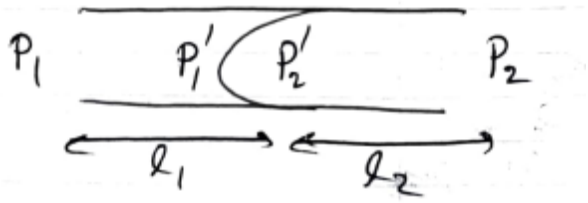

Figure 6: Pressures in a tube with two phases.

Let there be a higher pressure in P_1 than P_2, the fluid in node which has P_1 produces a meniscus which tends to move towards the second node. We can break it down into two separate tubes of lengths l_1 and l_2, containing fluid of viscosity μ_1 and μ_2. Then the flow rates for each of the tubes are given by:

$$Q_1 = \frac{\pi}{8\mu_1}\frac{P_1 - P_1^{'}}{l_1}R_1^4 \tag{17}$$

$$Q_2 = \frac{\pi}{8\mu_2}\frac{P_2^{'} - P_2}{l_2}R_2^4 \tag{18}$$

Multiplying equations 17 and 18 by $\mu_i l_i$

$$Q_1\mu_1 l_1 = \frac{\pi}{8}(P_1 - P_1^{'})R_1^4 \tag{19}$$

$$Q_2\mu_2 l_2 = \frac{\pi}{8}(P_2^{'} - P_2)R_2^4 \tag{20}$$

Due to continuity, which means no vacuum or fluid can be created, $Q_1 = Q_2$. Since it is the same tube, $R_1 = R_2$. Adding equation 19 and 20, we get:

$$Q(\mu_1 l_1 + \mu_2 l_2) = \frac{\pi}{8}R^4(P_1 - P_2 + P_2^{'} - P_1^{'}) \tag{21}$$

In figure 4 the water rises because there is a pressure jump at the meniscus, the pressure is lower on the side of the water. Therefore in our case $P_2^{'} - P_1^{'}$ will have a positive value. Equation 21 becomes:

$$Q = \frac{\pi R^4}{8(\mu_1 l_1 + \mu_2 l_2)}\left(\Delta P + \frac{2\sigma}{R}\right) \tag{22}$$

It is clear that $Q > Q'$, where Q' is the flow without the meniscus.

2.6 The sign of capillary pressure

Let the node on which we are generating linear equations be N_i and the node connected by a tube be N_j, if the concave side of the meniscus points towards N_j from N_i, then let us say that the meniscus points away from N_i or simply points away and in the case of opposite orientation points towards. Let the sign due to the orientation of meniscus be decided by a function called $s(d, n_{mns})$, where d is the direction or orientation, and n_{mns} is the number of meniscus in the tube:

$$s(d, n_{mns}) = \begin{cases} -1, & \text{points towards, } n_{mns} = 1 \\ 0, & n_{mns} = 0,\ 2 \\ +1, & \text{points away, } n_{mns} = 1 \end{cases} \tag{23}$$

Equation 22 can be written as:

$$Q = \frac{\pi R^4}{8(\mu_1 l_1 + \mu_2 l_2)} \left(\Delta P + \frac{2s\sigma}{R} \right) \tag{24}$$

The case when there are an even number of meniscus in a tube, the capillary pressures cancel each other out.

2.7 Flow rate equation used in our network model

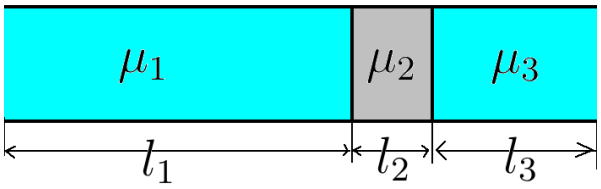

Figure 7: designation of viscosity and corresponding lengths of phases in a tube

Q_{ij} is the flow from N_i to N_j and $\Delta P_{ij} = P_i - P_j$.

$$\boxed{Q_{ij} = \frac{\pi R_{ij}^4}{8 M_{ij} l} \left(\Delta P_{ij} + \frac{2 s_{ij} \sigma}{R_{ij}} \right)} \tag{25}$$

Here M_{ij} is:

$$M_{ij} = \sum_k \mu_{ijk} \frac{l_{ijk}}{l}$$

It is clear that

$$Q_{ij} = -Q_{ji} \tag{26}$$

2.8 Set of linear equations for a node

Let us apply our method on a simple system consisting of only 5 nodes. Note that all Q point outward. It is only to denote the direction. In order to preserve the law of conservation of volume, the Q's will have different signs.

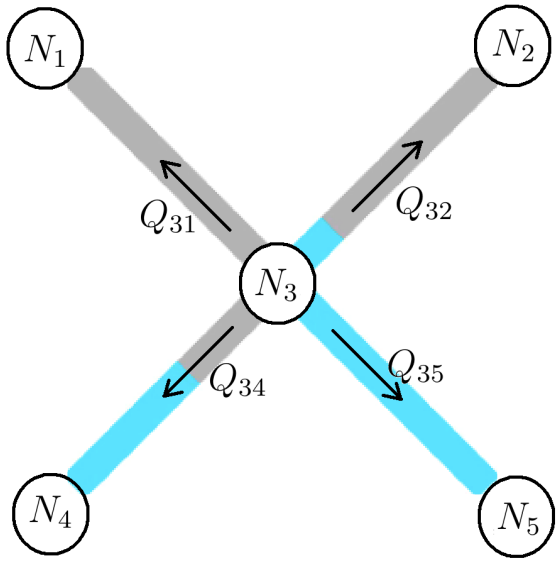

Since there are 4 tubes, we can write 4 equations according to 25

$$Q_{31} = \frac{\pi R_{31}^3}{8lM_{31}}(R_{31}\Delta P_{31} + 2s_{31}\sigma)$$

$$Q_{32} = \frac{\pi R_{32}^3}{8lM_{32}}(R_{32}\Delta P_{32} + 2s_{32}\sigma)$$

$$Q_{34} = \frac{\pi R_{34}^3}{8lM_{34}}(R_{34}\Delta P_{34} + 2s_{34}\sigma)$$

$$Q_{35} = \frac{\pi R_{35}^3}{8lM_{35}}(R_{35}\Delta P_{35} + 2s_{35}\sigma)$$

Due to the conservation of volume, we have:

$$\sum_k Q_{3k} = 0$$

Where $k = 1, 2, 4, 5$.

3 Features and Characterstics of our Model

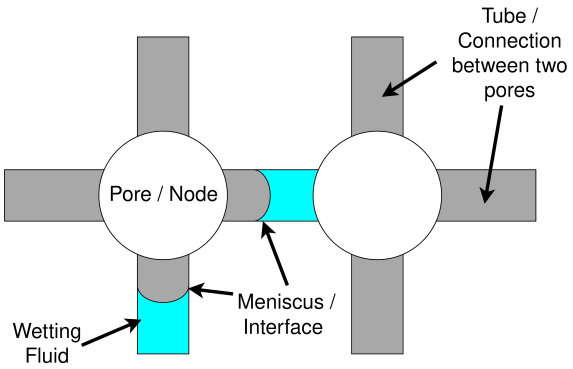

Figure showing two nodes from the network where the size of the node is much larger than the radius such that the capillary force tends to zero when the meniscus enters a node. In our model the volume of the pore is not taken into consideration. And all the capillaries which are denoted as tubes are cylindrical. All tubes are of equal length for simplicity.

3.1 Numbering tubes and other parameters in the network model

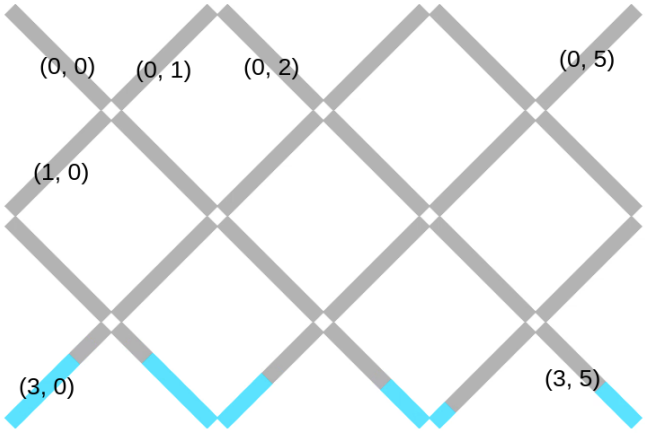

Figure 8: Numbering of tubes for a (rows, cols) = (4, 6) network model

If X is a parameter then X_{ij} is on the i th row and j th column, note that counting begins from zero. This type of counting is suitable for std::vector¡ data structure in C++.

3.2 Linear equations for simple displacement

In our model a node is connected to 4 tubes, or less if the node is located at the edges or a corner. The two-dimensional model can be extended to a three-

dimensional case similar to [25].

When generating the linear equations. For each row it is necessary to do the following for each direction:

$$[P_i] = [P_i] + R_{ij}K_{ij}$$
$$[P_j] = [P_j] - R_{ij}K_{ij}$$
$$[const] = [const] - 2s_{ij}\sigma K_{ij}$$

Here let $K_{ij} = R_{ij}^3/M_{ij}$.

For simplicity we rewrite the system of four equations as

In case of 5 nodes in our system, where the pressure of the bottom and top nodes are given and fixed, the matrix for Gaussian elimination will be:

$$\begin{pmatrix} 1 & 0 & 0 & 0 & 0 & P_{up} \\ 0 & 1 & 0 & 0 & 0 & P_{up} \\ -R_{31}K_{31} & -R_{32}K_{32} & (R_{3k}K_{3k}+...) & -R_{34}K_{34} & -R_{35}K_{35} & -2\sigma(s_{3k}K_{3k}+...) \\ 0 & 0 & 0 & 1 & 0 & P_{down} \\ 0 & 0 & 0 & 0 & 1 & P_{down} \end{pmatrix}$$

It can be proven that this matrix always has a solution. Once the solution is determined the flow rate can be calculated using equation 25, and the velocity of flow in each tube is given by

$$\boxed{v_{ij} = \frac{R_{ij}}{8lM_{ij}}(R_{ij}\Delta P_{ij} + 2s_{ij}\sigma)} \tag{27}$$

3.3 Linear equations in case of infinitely many solutions

It is possible to calculate the pressures at each node, if the pressures are known on the edges. However when we want to model imhibition, the boundaries are closed and the total volume of a phase remains the same.

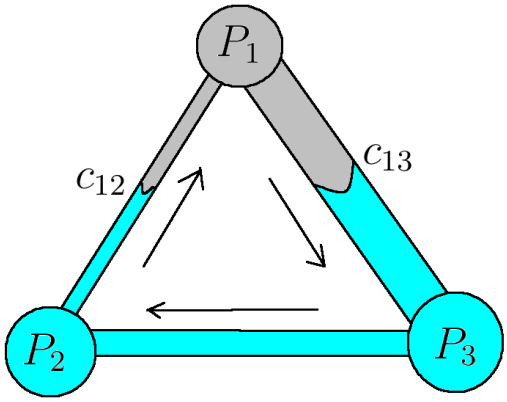

Figure 9: Case of of infinitely many solutions

Let the flow rates be given by:

$$q_{ij} = k_{ij}\Delta P + c_{ij} \tag{28}$$

For N_1:

$$q_{12} = k_{12}(P_1 - P_2) + c_{12}$$
$$q_{13} = k_{13}(P_1 - P_3) + c_{13}$$

Since:

$$q_{12} + q_{13} = 0$$
$$(k_{12} + k_{13})P_1 - k_{12}P_2 - k_{13}P_3 = -c_{12} - c_{13}$$

Then for each node we obtain the following matrix:

$$\begin{pmatrix} (k_{12}+k_{13}) & -k_{12} & -k_{13} & -c_{12}-c_{13} \\ -k_{21} & (k_{21}+k_{23}) & -k_{23} & -c_{21}-c_{23} \\ -k_{31} & -k_{32} & (k_{31}+k_{32}) & -c_{31}-c_{32} \end{pmatrix}$$

Note that:

$$k_{ij} = k_{ji}$$
$$c_{ij} = -c_{ji}$$

Hence the sum of each column of this matrix is zero.

By $R_3 = R_3 + R_1 + R_2$:

$$\begin{pmatrix} (k_{12}+k_{13}) & -k_{12} & -k_{13} & -c_{12}-c_{13} \\ -k_{21} & (k_{21}+k_{23}) & -k_{23} & -c_{21}-c_{23} \\ 0 & 0 & 0 & 0 \end{pmatrix}$$

This is solved by adding a constant a to one of the column of the matrix for each rows. In our model the centre was chosen to be the zero of pressure. Changing this point does not change the flow rates or the nature of flows.

$$\begin{pmatrix} (k_{12}+k_{13}) & -k_{12} & -k_{13}+a & -c_{12}-c_{13} \\ -k_{21} & (k_{21}+k_{23}) & -k_{23}+a & -c_{21}-c_{23} \\ -k_{31} & -k_{32} & (k_{31}+k_{32})+a & -c_{31}-c_{32} \end{pmatrix}$$

After $R_3 = R_3 + R_1 + R_2$:

$$\begin{pmatrix} (k_{12}+k_{13}) & -k_{12} & -k_{13}+a & -c_{12}-c_{13} \\ -k_{21} & (k_{21}+k_{23}) & -k_{23}+a & -c_{21}-c_{23} \\ 0 & 0 & 3a & 0 \end{pmatrix}$$

$$3aP_3 = 0$$

The solutions exists only if $P_3 = 0$.

3.4 Distribution and recombination

The novelty of our model is how we distribute phases in the nodes. When more than two phases flow into a node, the wetting fluid first enters the tube with the thinner radius. Our data structure was constrained to only allow the case for a maximum of two meniscus in a tube.

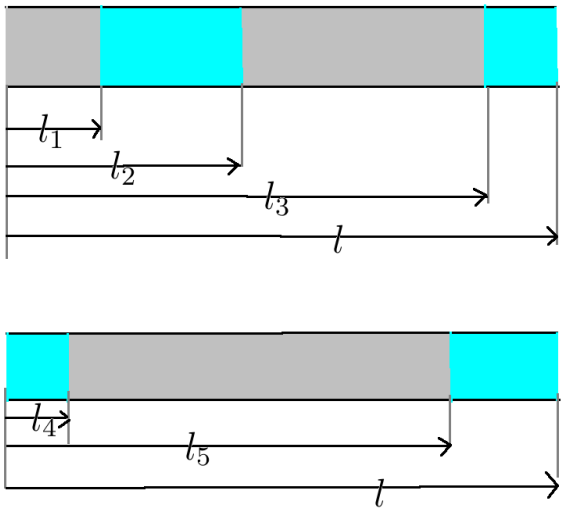

Figure 10: Case of more than two meniscus in a tube

Grey: $m_1 = l_1$ at $d_1 = \frac{l_1}{2}$,

$m_2 = l_3 - l_2$ at $d_2 = \frac{(l_3+l_2)}{2}$

$$m = m_1 + m_2$$
$$c_{grey} = \frac{m_1 d_1 + m_2 d_2}{m}$$

$$l_4 = c_{grey} - \frac{m}{2}$$
$$l_5 = l_4 + m$$

3.5 Algorithm for computation

1. **Input Files:** read input files, radius.txt and mns.txt, mns.txt contains the initial setup of the meniscus
2. **Random radius:** add very small random values to the radius, this is done in order to remove the case of two equal radius for simplicity, can be removed later
3. **Loop time:** do until a certain proportion of invading fluid is reached for example 0.90 or a fixed number of frames:
   (a) **Pressure:** determine the pressure at each node using the linear equations given in section 2.8.
   (b) **Velocity:** Calculate the velocity using equation 27
   (c) **time step:** determine the time step, it is the $\Delta t = minl/vi$.
   (d) **volume:** The volume displaced in each tube is determined by iterating through all the tubes, $V_{ij} = v_{ij} * t_{min}$.
   (e) **integration:**
      i. **Store insertion:** create a matrix to store how much of which fluid to insert in each of these tubes.
      ii. **Loop nodes:** Iterate through all the nodes, and for each of the nodes.
         A. divide the tubes into two categories, flow-in-tube - here the fluid from these tubes flow into the nodes, flow-out-tubes here we insert the fluid into the tube from the node
         B. Find out the total of fluid1, fluid2, which is the total of each fliud from all flow-in-tubes.
         C. Start filling the each of the flow-out-tubes where the flow will go into in ascending order of the radius of the tube. This will be done simply be adding the quantity of fluid1 and fluid2 to the matrix created above.

D. while filling fist use fluid1, once fluid1 is used up then start using fluid2, which means if in a tube we have to insert two fluids, then fluid1 will go in first.

iii. **Fluid addition:** For each of the tubes, add the volume of fluid determined to be added. After addition if there are more than 2 meniscus, then merge them retaining their center of masses.

(f) **Picture:** Save a picture of the current configuration.

4. Video: Make a video file from the pictures.

3.6 Possible Cases of Errors

3.6.1 Initial configuration for flow to start

The flow did not start when all the meniscus were located inside the nodes. Because in our model we assumed that there is not capillary pressure in the nodes. To overcome this, the meniscus were made to be situated inside the tubes.

3.6.2 Case of all meniscus located in the thick tubes

The solution of linear equation were such that, the capillary force balanced out the pressure gradient. The pressure was much higher outside in the thick tubes than in the thin tubes. Whether this was caused by error in the process of solving the linear equation or due to the initial setup, needs to be checked again. Error is, that it is impossible to determine whether the coefficient during the process of gauss elimination is zero or not. Because of the way how floating point numbers are handled by the CPU, 0 is often seen as a small number.

3.7 Simple tests for our model

3.7.1 Filtration

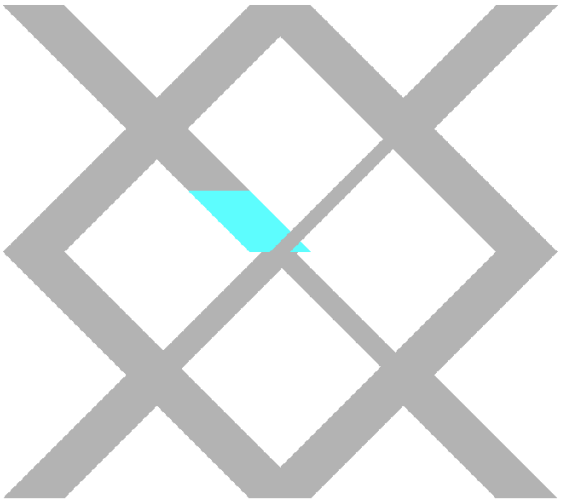

Figure 11: Initial position of wetting fluid

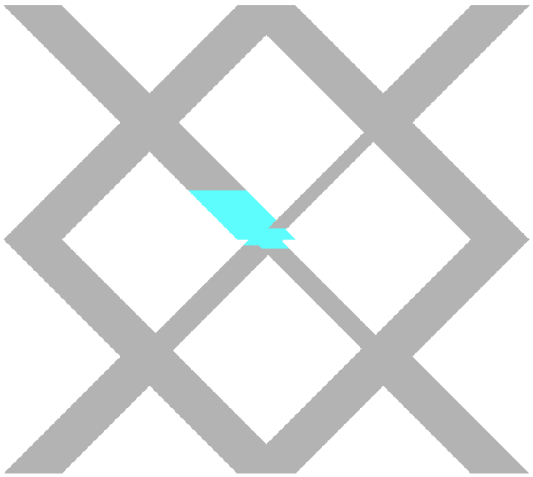

Figure 12: The wetting fluid chose to move to the tubes with thinner radius.

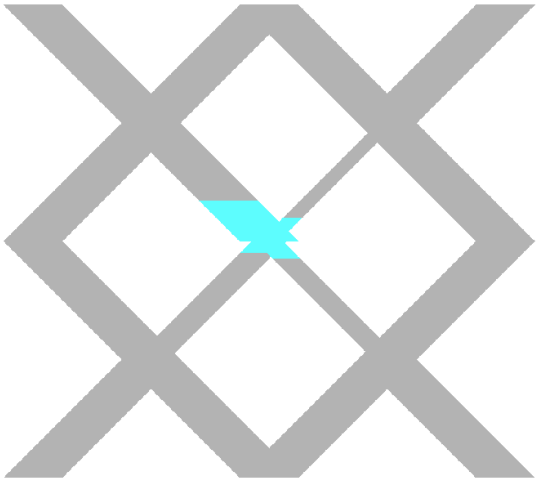

Figure 13: The flow accelerates as more fluid is in the thinner radius, here viscosity of the wetting fluid is higher.

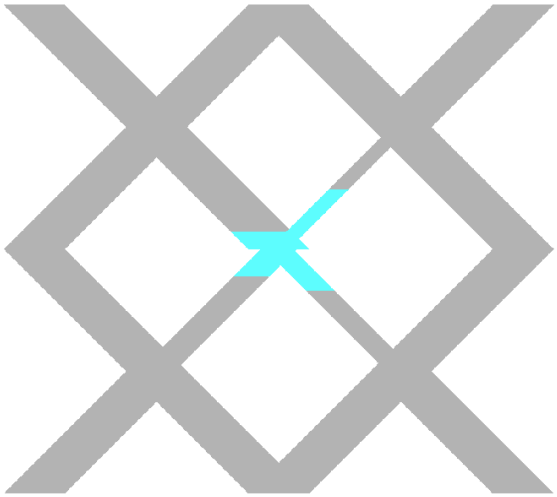

Figure 14

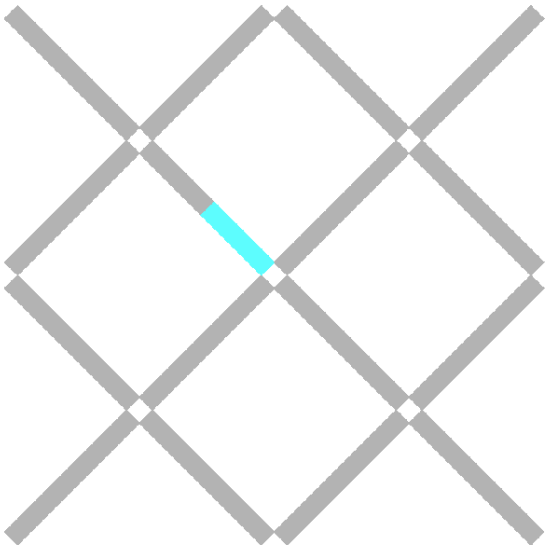

Figure 15: The same flow without plotting the radius thickness for clarity.

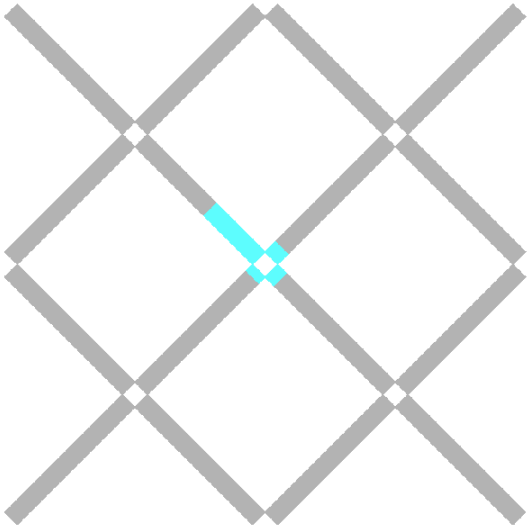

Figure 16

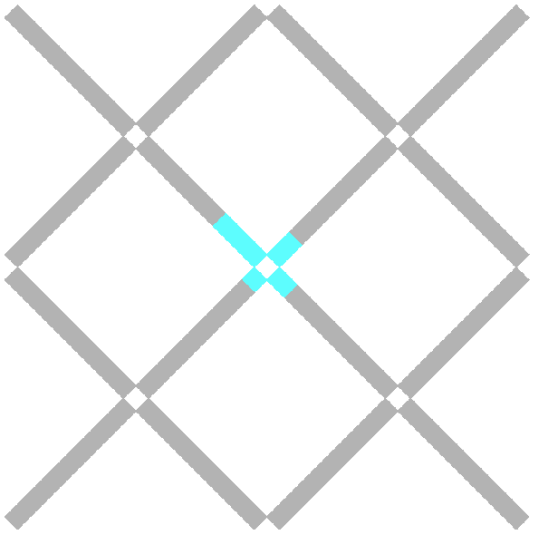

Figure 17

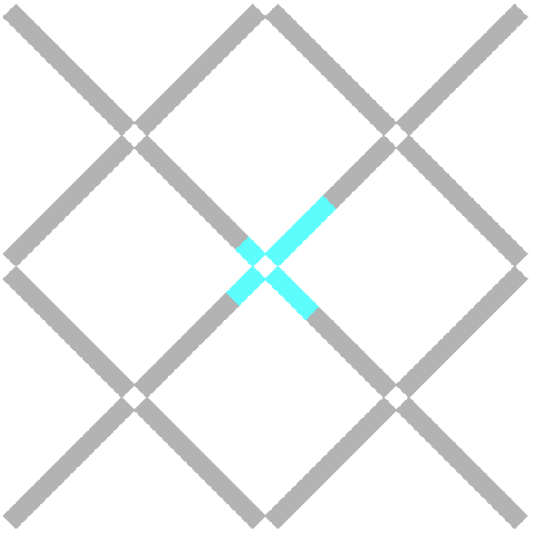

Figure 18

3.7.2 Displacement

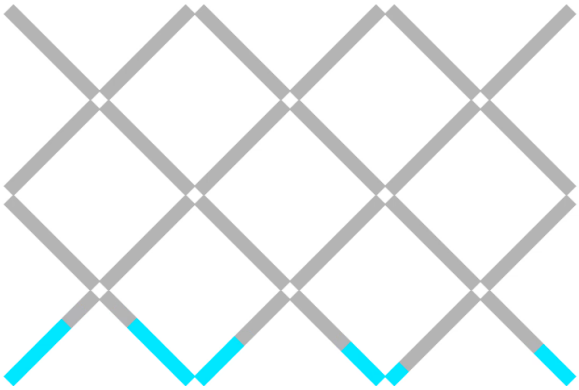

Figure 19: Our model is initially set up such that the wetting fluid is low in saturation and is confined to the bottom of our network. A higher pressure is fixed for all nodes at the bottom layer, while a low pressure is fixed for the top row.

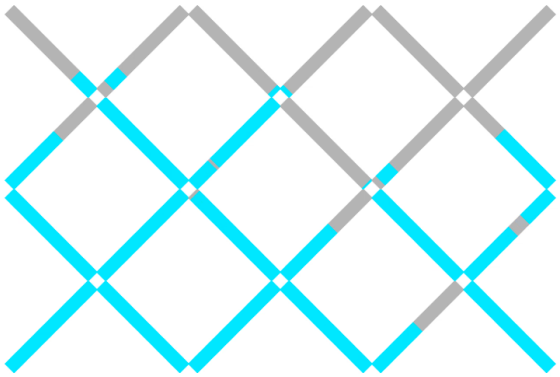

Figure 20: In all nodes, law of conservation of volume is applied, since mass is conserved and the phases are non-compressible. However for the bottom layer of nodes, the wetting fluid is injected as much required according to the sum of flow rates determined in the tubes connected to those nodes, while from the top layer of nodes a fluid is removed.

4 Simulation

4.1 Main Problem

- The aim of this simulation is observe the movement of wettable fluid (blue) from the region of thicker tube to the thinner tube.
- The saturation of each phase is measured in the region of thinner tubes.

- All boundaries are closed, the saturation of a phase for the whole system remains constant in time.
- The radius in the outer region is three times larger.

4.2 Result for Imbibition 10x10

4.2.1 Figures

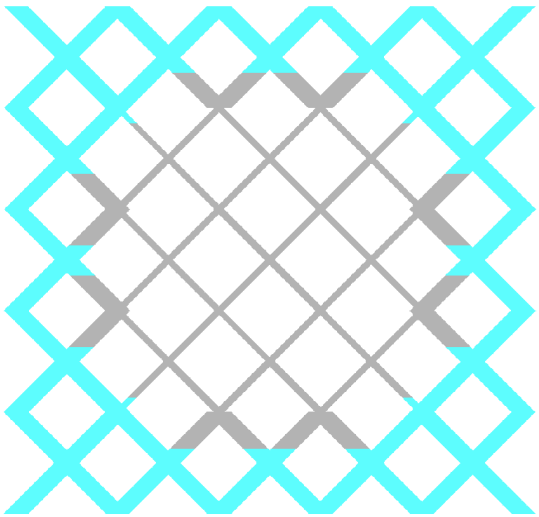

Figure 21: Initial setup, outer radius is 3 times larger than inner.

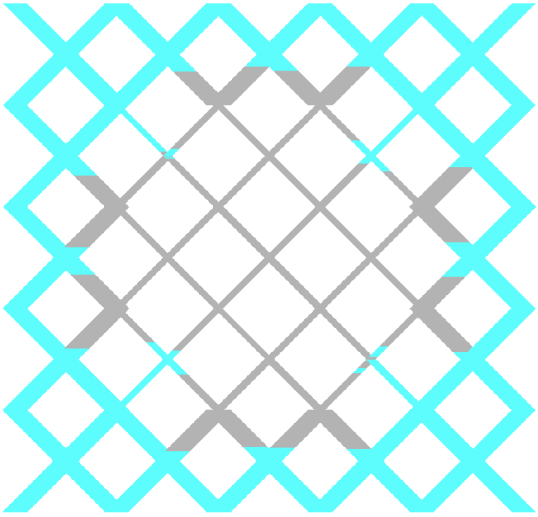

Figure 22: Showing invasion of wetting(blue) fluid into the region which contains thinner radius. The flow accelerates because, for a corner initially there are 3 meniscus, it multiplies into 3 when the meniscus reaches the node. The corner where the meniscus reaches the node late is pushed back because of the excessive pressures from the other corners.

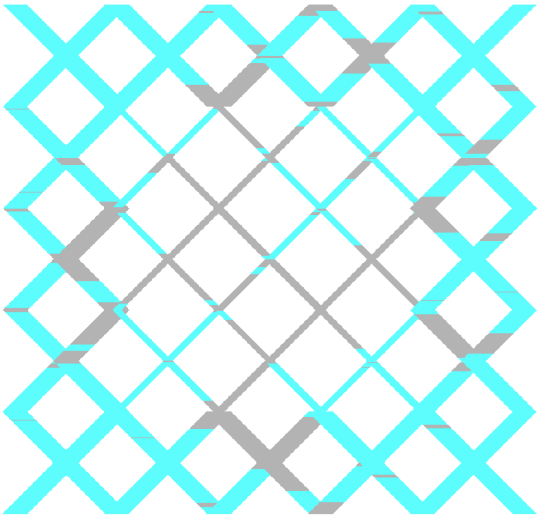

Figure 23: The invasion slows down and possibly oscillates, it is due to the meniscus in the inner region being ineffective to suck more blue fluid as most tubes have two meniscus. In our algorithm, tubes with two meniscus have a zero net pressure.

4.2.2 Plot

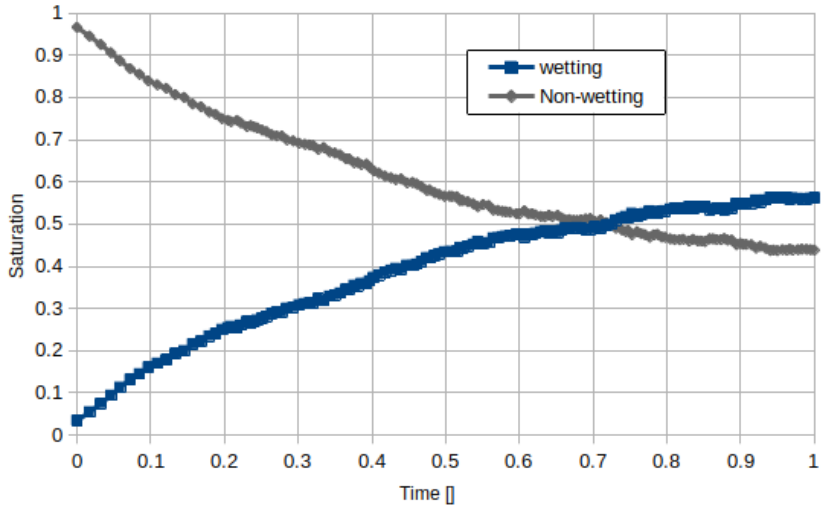

Figure 24: Plot of saturation of blue fluid in the region of thinner radius with respect to time, here the time is without dimensions.

For the simulations the length of each tube was taken to be unity and only the ratio of viscosity was used in equation 25, since these values do not change the geometry of the flow and change only the scale of time. Dimensionless value of time was used.

4.2.3 Discussion

1. The blue fluid has approximately logarithmic dependence with time, the invasion rapidly rises and slows down, until it becomes almost constant. The calculation was stopped after 150 steps, because there was very small progress after it. Note that the time step for each step is different.
2. The blue fluid enters up to 0.56 of the saturation.
3. The saturation vs time appears similar to the ones in the reference [2], [8].

4.3 Result for Imbibition 26x26

4.3.1 Figures

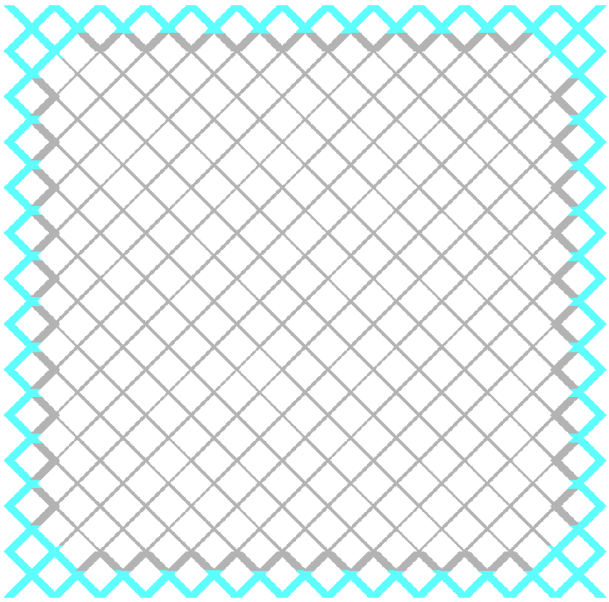

Figure 25: Initial setup

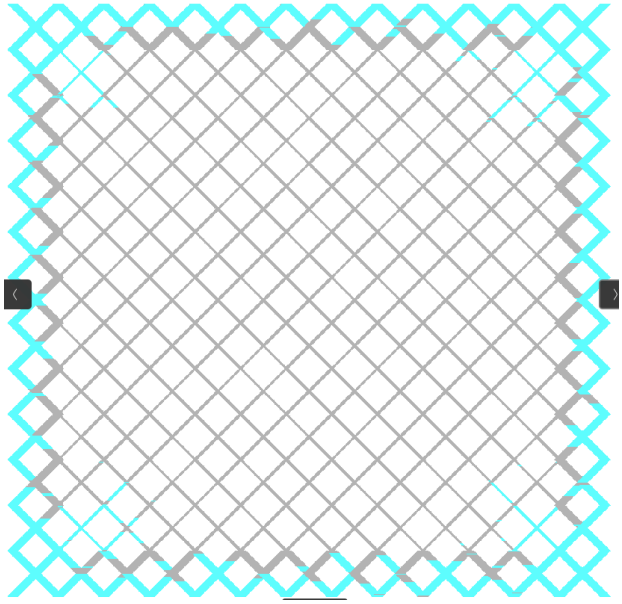

Figure 26: Acceleration

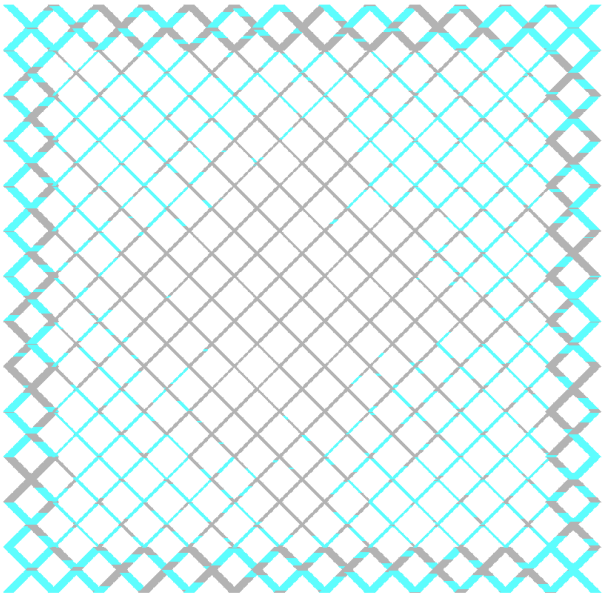

Figure 27: Slowing down

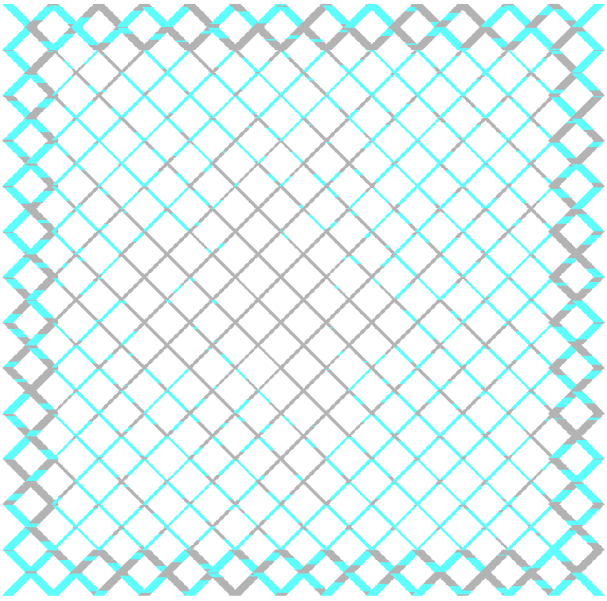

Figure 28: Final

4.3.2 Plot

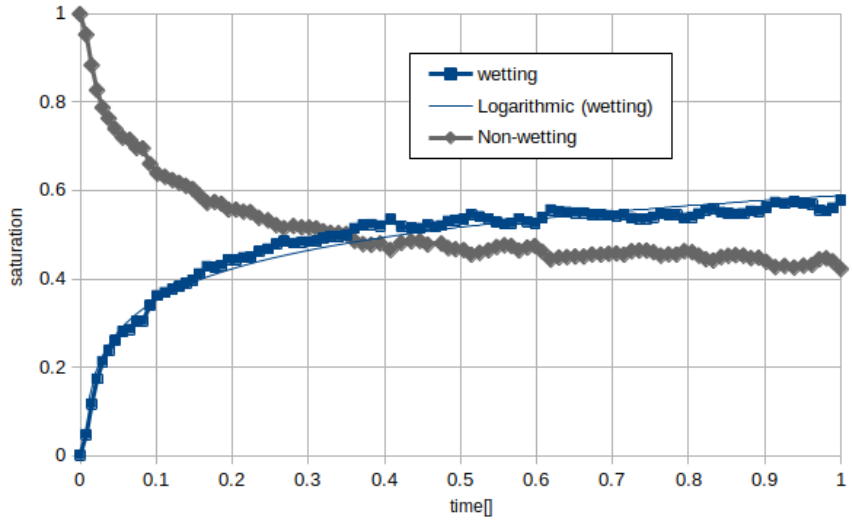

Figure 29: Plot of saturation of blue fluid in the region of thinner radius with respect to dimensionless time.

4.3.3 Discussion

1. Calculation was done for 20,000 steps.
2. Plot for every 200 frames.
3. Equal volumes of each phases.
4. The saturation for wetting fluid is 0.57 for the inner region, which is very close the previous simulation for 10x10.
5. It is clear that the relaxation parameter is present as the saturation converges to an equilibrium value.

5 Conclusion

1. The saturation of a phase in the inner region of the porous body tends to an equilibrium value.
2. The method of distributing fluid such the wetting fluid first goes to the tube with the thinner radius and calculating the flow rate using the modified Poiseuille equation is valid for explaining relaxation phenomena.
3. This algorithm can be extended to the case where there are more than 4 tubes connected to a node, since for two phase flow into a node case, we distribute in an ascending order of radii, in our model it is distributed to a maximum number to two tubes, but for hexagonal model it can be 4. We only need to update the function which produces the connections. The

same model can be used for a 3-dimensional case, where one surface has higher pressure than the opposite surface which has a lower pressure, it is to be used in order to more accurately represent the porous body.

4. Model of reasonable size can be simulated using Gaussian-elimination, which is more accurate than iterative methods.

5. The total volume for each phase for the whole system remains the same with the accuracy of 10^{-9}. Use of double is recommended instead of float.

6. Changing the ratio of viscosity affects the rate of displacement in the presence of pressure gradient, however in the case of inbibition significant differences were not observed.

7. The work will be continued as a part of Master's thesis. The ultimate goal is to verify the Kondaurov model, determine the physical meaning of the non equilibrium parameter, and the scope of its applicability.

References

[1] Cyrus K Aidun and Jonathan R Clausen. Lattice-boltzmann method for complex flows. *Annual review of fluid mechanics*, 42:439–472, 2010.

[2] Eyvind Aker, Knut JØrgen MÅlØy, Alex Hansen, and G George Batrouni. A two-dimensional network simulator for two-phase flow in porous media. *Transport in porous media*, 32:163–186, 1998.

[3] GI Barenblatt, TW Patzek, and DB Silin. The mathematical model of nonequilibrium effects in water-oil displacement. *SPE journal*, 8(04):409–416, 2003.

[4] Grigory I Barenblatt, Iu P Zheltov, and IN Kochina. Basic concepts in the theory of seepage of homogeneous liquids in fissured rocks [strata]. *Journal of applied mathematics and mechanics*, 24(5):1286–1303, 1960.

[5] Maria C Bravo and Mariela Araujo. Analysis of the unconventional behavior of oil relative permeability during depletion tests of gas-saturated heavy oils. *International journal of multiphase flow*, 34(5):447–460, 2008.

[6] Jing-Den Chen and David Wilkinson. Pore-scale viscous fingering in porous media. *Physical review letters*, 55(18):1892, 1985.

[7] Shiyi Chen and Gary D Doolen. Lattice boltzmann method for fluid flows. *Annual review of fluid mechanics*, 30(1):329–364, 1998.

[8] I Fatt. The network model of porous media. 3. dynamic properties of networks with tube radius distribution. *Transactions of the American institute of mining and metallurgical engineers*, 207(7):164–181, 1956.

[9] Yanbin Gong. *Dynamic Pore Network Modeling of Two-Phase Flow and Solute Transport in Disordered Porous Media and Rough-Walled Fractures*. University of Wyoming, 2021.

[10] S Majid Hassanizadeh. Continuum description of thermodynamic processes in porous media: Fundamentals and applications. *Modeling Coupled Phenomena in Saturated Porous Materials*, pages 179–223, 2004.

[11] S Majid Hassanizadeh, Michael A Celia, and Helge K Dahle. Dynamic effect in the capillary pressure–saturation relationship and its impacts on unsaturated flow. *Vadose Zone Journal*, 1(1):38–57, 2002.

[12] S Majid Hassanizadeh and William G Gray. High velocity flow in porous media. *Transport in porous media*, 2:521–531, 1987.

[13] S Majid Hassanizadeh and William G Gray. Mechanics and thermodynamics of multiphase flow in porous media including interphase boundaries. *Advances in water resources*, 13(4):169–186, 1990.

[14] S Majid Hassanizadeh and William G Gray. Thermodynamic basis of capillary pressure in porous media. *Water resources research*, 29(10):3389–3405, 1993.

[15] M King Hubbert. Darcy's law and the field equations of the flow of underground fluids. *Transactions of the AIME*, 207(01):222–239, 1956.

[16] V Joekar-Niasar, S Majid Hassanizadeh, and HK Dahle. Non-equilibrium effects in capillarity and interfacial area in two-phase flow: dynamic pore-network modelling. *Journal of fluid mechanics*, 655:38–71, 2010.

[17] PR King. The fractal nature of viscous fingering in porous media. *Journal of Physics A: Mathematical and General*, 20(8):L529, 1987.

[18] VI Kondaurov. The thermodynamically consistent equations of a thermoelastic saturated porous medium. *Journal of applied mathematics and mechanics*, 71(4):562–579, 2007.

[19] VI Kondaurov. A non-equilibrium model of a porous medium saturated with immiscible fluids. *Journal of Applied Mathematics and Mechanics*, 73(1):88–102, 2009.

[20] Andrey Konyukhov, Leonid Pankratov, and Anton Voloshin. The homogenized kondaurov type non-equilibrium model of two-phase flow in multiscale non-homogeneous media. *Physica Scripta*, 94(5):054002, 2019.

[21] N Labed, L Bennamoun, and JP Fohr. Experimental study of two-phase flow in porous media with measurement of relative permeability. *Fluid Dyn. Mater. Process*, 8(4):423–436, 2012.

[22] Stephen B Pope and Stephen B Pope. *Turbulent flows*. Cambridge university press, 2000.

[23] Harris Sajjad Rabbani. *Pore-scale investigation of wettability effects on two-phase flow in porous media*. The University of Manchester (United Kingdom), 2018.

[24] Amir Raoof and S Majid Hassanizadeh. A new method for generating pore-network models of porous media. *Transport in porous media*, 81:391–407, 2010.

[25] Santanu Sinha, Andrew T Bender, Matthew Danczyk, Kayla Keepseagle, Cody A Prather, Joshua M Bray, Linn W Thrane, Joseph D Seymour, Sarah L Codd, and Alex Hansen. Effective rheology of two-phase flow in three-dimensional porous media: experiment and simulation. *Transport in porous media*, 119:77–94, 2017.

[26] Cameron Tropea, Alexander L Yarin, John F Foss, et al. *Springer handbook of experimental fluid mechanics*, volume 1. Springer, 2007.

[27] Grétar Tryggvason, Bernard Bunner, Asghar Esmaeeli, Damir Juric, N Al-Rawahi, W Tauber, J Han, S Nas, and Y-J Jan. A front-tracking method for the computations of multiphase flow. *Journal of computational physics*, 169(2):708–759, 2001.

[28] Markus Uhlmann. An immersed boundary method with direct forcing for the simulation of particulate flows. *Journal of computational physics*, 209(2):448–476, 2005.

[29] Per H Valvatne and Martin J Blunt. Predictive pore-scale modeling of two-phase flow in mixed wet media. *Water resources research*, 40(7), 2004.

[30] Edward W Washburn. The dynamics of capillary flow. *Physical review*, 17(3):273, 1921.

[31] Wikipedia. Capillary action — Wikipedia, the free encyclopedia. `http://en.wikipedia.org/w/index.php?title=Capillary%20action&oldid=1155129318`, 2023. [Online; accessed 19-June-2023].

[32] Wahyu Perdana Yudistiawan, Sang Kyu Kwak, and Santosh Ansumali. Higher order galilean invariant lattice boltzmann model. In *The 6th International Conference for Mesoscopic Methods in Engineering and Science*, page 28, 2009.